Construction and Building Materials 124 (2016) 961–966

Contents lists available at ScienceDirect

Construction and Building Materials

journal homepage: www.elsevier.com/locate/conbuildmat

Technical note

Synthesizing one-part geopolymers from rice husk ash

P. Sturm [a], G.J.G. Gluth [a,*], H.J.H. Brouwers [b], H.-C. Kühne [a]

[a] Division 7.4 Technology of Construction Materials, Bundesanstalt für Materialforschung und -prüfung (BAM), Berlin, Germany
[b] Department of the Built Environment, Eindhoven University of Technology, Eindhoven, The Netherlands

ARTICLE INFO

Article history:
Received 20 June 2016
Received in revised form 5 August 2016
Accepted 7 August 2016
Available online 11 August 2016

Keywords:
Alkali-activation
Geopolymers
One-part formulation
Bio-based materials
Rice husk ash

ABSTRACT

One-part geopolymers offer advantages over conventional geopolymers with regard to handling and storage of feedstocks. However, they often suffer from a low degree of reaction, a high amount of crystalline byproducts, and consequently low strength. In this study, one-part geopolymers were produced from rice husk ash (RHA) and sodium aluminate, and investigated by XRD, ATR-FTIR, SEM and compressive strength testing. The compressive strength of the material was ~30 MPa, i.e. significantly higher than for comparable one-part geopolymers. This is attributed to an almost complete reaction of the RHA and the absence of crystalline byproducts (zeolites) in the hardened geopolymer.

1. Introduction

Because of their versatile potential, conventional "two-part" geopolymers, synthesized by activation of solid aluminosilicate feedstocks (e.g., metakaolin, fly ash and blast-furnace slag) with highly alkaline liquids (e.g., sodium hydroxide and sodium silicate solutions), have been subject of a large number of studies in the last decades (e.g. [1–10]). More recent approaches have focused on so called "one-part" formulations. For this route the alkaline activator is provided in solid form and just water has to be added to initiate the geopolymerization reactions and hardening ("just add water geopolymers") [11,12]. In these formulations the activator solution forms directly in the reaction system, thus the synthesis procedure is comparable to that for the hydration of ordinary Portland cement (OPC)-based binder systems. With this approach handling of highly alkaline solutions and problems with aging of these solutions are avoided, which can provide a better social and economic acceptance [12,13]. However, the investigated one-part systems are often dominated by crystalline tectosilicates (zeolites) and the reported compressive strengths are usually lower than for conventional two-part geopolymers [11,12,14–19].

Rice husk ash (RHA) is a silica-rich agriculture waste material, typically consisting of 90–95 wt.% amorphous SiO_2 [20]. In 2010 over 700 million tons of rice were produced worldwide [21] in a context of a steadily increasing demand. This translates to a production of about 140 million tons of husk in 2010. Calcination of the husks leaves about 25 wt.% of the initial mass as ash, the so-called RHA [22]. Highly reactive, amorphous RHAs can be produced at calcination temperatures up to 800 °C [23–26], which is significantly below the temperatures for the production of conventional OPC clinkers. Heating at higher temperatures is not beneficial because it leads to the formation of crystalline cristobalite and tridymite in the ash [24], which decreases its reactivity. RHA has been investigated for its use in various industrial applications including the use as supplementary cementitious material for conventional cement based binder systems (e.g. [27–29]). Recent studies investigated the production of sodium silicate solutions from RHA for use as activating solution for conventional "two part" geopolymers [30–33].

In this communication we report on the use of RHA as solid precursor in the production of one-part geopolymers. The results show that the RHA is highly reactive and is able to form a typical geopolymer gel with higher compressive strength than is generally observed for one-part geopolymers.

2. Materials and methods

2.1. Materials

The starting materials were characterized by inductively coupled plasma optical emission spectroscopy (ICP-OES), X-ray diffraction (XRD), attenuated total reflection Fourier transform infrared spectroscopy (ATR FT-IR) and scanning electron

* Corresponding author.
E-mail address: gregor.gluth@bam.de (G.J.G. Gluth).

http://dx.doi.org/10.1016/j.conbuildmat.2016.08.017
0950-0618/

microscopy (SEM). The experimental conditions are described in Section 2.3.

The employed rice husks from Tanzania were calcined at 650 °C for 90 min to yield the rice husk ash (RHA) and the ash then allowed to cool down naturally to room temperature. After cooling, the RHA was ground in a disc mill for 18 s. Particles that did not pass a sieve with 63 μm mesh size were ground for further 18 s; after the second milling all particles passed the applied sieve.

The particle size distribution (PSD) of the RHA was investigated using laser granulometry (Fig. 1). The median of the PSD was determined to be d_{50} = 11.1 μm (and d_{90} = 39.8 μm), which is in line with SEM micrographs of the RHA (Fig. 2). The BET specific surface area of the RHA was determined to be 49.6 m^2/g (average pore diameter ~12.9 nm), using N_2 sorption at 77 K. An apparent particle density of 2.259 ± 0.003 g/cm^3 was determined by He pycnometry.

The RHA contained 88.49 wt.% SiO_2 (Table 1). XRD showed a major amorphous hump, centered at ~22° 2θ, and minor amounts of the following crystalline impurities: quartz (PDF # 00-046-1045), potassium magnesium phosphate (PDF # 00-050-0146), cristobalite (PDF # 00-039-1425), and calcite (PDF # 01-086-0174) (Fig. 3).

The employed sodium aluminate ($NaAlO_2$) had an almost stoichiometric Na/Al ratio of nearly unity (1.001 mol/mol; cf. Table 1). Besides anhydrous sodium aluminate (PDF # 00-033-1220), XRD also indicated minor amounts of hydrated sodium aluminate (PDF # 01-083-0315) and natrite (PDF # 01-072-0628). This is in agreement with the low loss on ignition of 2.63 wt.% (Table 1) and the tendency of alkaline compounds to carbonate.

2.2. Geopolymer synthesis

One-part geopolymers were synthesized by mixing RHA and solid sodium aluminate, and subsequently adding water at a nominal water/binder ratio (w/b) of 0.5 by mass to yield molar Na_2O:Al_2O_3:SiO_2:H_2O ratios as presented in Table 2. The alkaline activator was provided as the sodium aluminate, which dissolves readily in water, thus water only had to be added to initiate the reactions. The mix-design was chosen to facilitate comparison with previously investigated formulations with the same molar ratios [16,18,19].

Pastes were mixed for 4 min using a contact free planetary centrifugal mixer at a rotation speed of 1200 min^{-1}. After mixing the pastes were immediately cast into 20 mm × 20 mm × 20 mm cube moulds. The samples were cured in the open moulds at 80 °C and 80% r.H. in an oven with climate (r.H.) conditioning. The curing temperature of 80 °C was chosen to accelerate geopolymerization reactions and hardening, as is standard in geopolymer technology (e.g. [4,5,12,18,30]), though geopolymers from highly reactive feedstocks in an optimized mix can also be cured at room

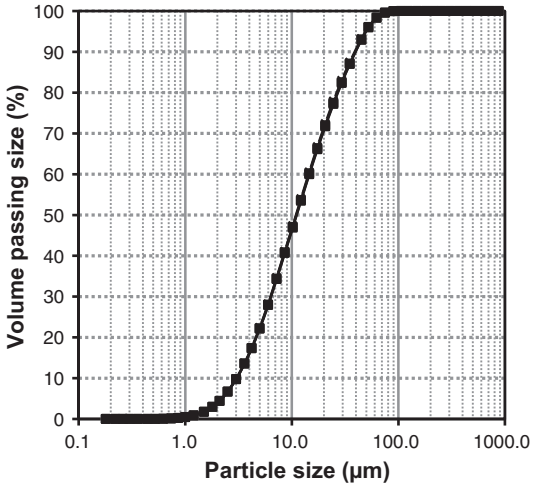

Fig. 1. Particle size distribution of the rice husk ash.

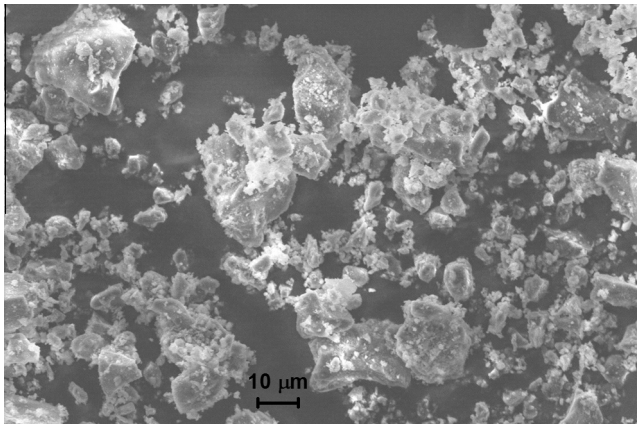

Fig. 2. SEM micrograph of the rice husk ash.

Table 1
Chemical composition of the starting materials.

Component	RHA	$NaAlO_2$
	(wt.%)	(wt.%)
SiO_2	88.49	<0.01
Al_2O_3	0.58	59.74
Fe_2O_3	0.31	0.02
TiO_2	0.03	<0.01
CaO	1.00	0.39
MgO	0.88	0.01
Na_2O	0.24	36.35
K_2O	2.91	0.01
SO_3	0.54	0.04
P_2O_5	1.83	n.d.
LOI	2.48	2.63

n.d.: not determined; LOI: loss on ignition at 1000 °C.

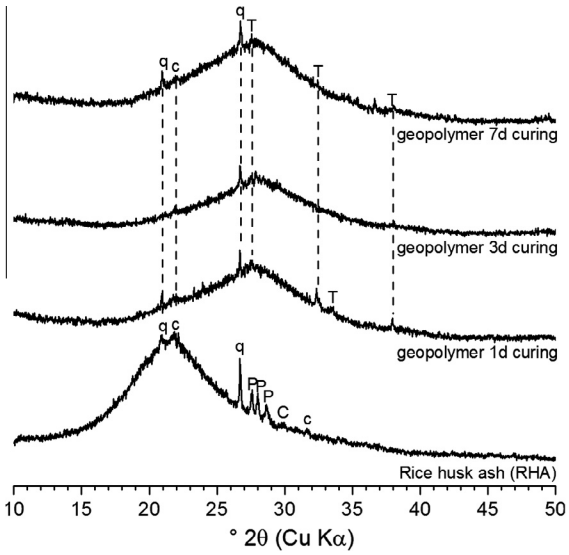

Fig. 3. XRD patterns of the RHA feedstock and the one-part geopolymers after 1 d, 3 d and 7 d of curing. (q = quartz, c = cristobalite, P = potassium magnesium phosphate; C = calcite, T = thermonatrite.).

Table 2
Mix-design and molar ratios of the one-part geopolymers.

m(Na_2O) (wt.%)	m(Al_2O_3) (wt.%)	m(SiO_2) (wt.%)	m(H_2O) (wt.%)	Na_2O/Al_2O_3 (mol/mol)	SiO_2/Al_2O_3 (mol/mol)	H_2O/Al_2O_3 (mol/mol)
10.17	16.76	34.46	35.03	1.00	3.48	11.81

temperature in a reasonable time [6,9,10,15]. After the desired curing times (24 h, 3 d or 7 d) the specimens were removed from the oven and the moulds, allowed to cool down to room temperature, and tested according to the procedures described in Section 2.3. Curing times longer than 24 h are unusual in geopolymer technology and would require higher energy consumption; nevertheless, longer curing times were investigated to clarify whether these can improve the mechanical properties of the material.

2.3. Structural and mechanical investigations

XRD investigations were conducted on powdered samples on a Rigaku Ultima IV device using the following measurement conditions: Bragg-Brentano geometry; CuKα radiation (λ = 1.5419 Å); scanning range: 5–65° 2θ; step size: 0.02° 2θ; scanning speed: 0.5° 2θ min^{-1}; sample rotation speed: 15 rpm.

ATR FT-IR experiments were performed on powdered samples on a Bruker Tensor 27 device with a diamond ATR module. Spectra were recorded in the range 4000–400 cm^{-1} with a resolution of 4 cm^{-1} and 16 scans per spectrum (detector: RT-DLaTGS).

SEM observations were carried out on a Carl Zeiss EVO MA10 device at an accelerating voltage of 7–10 kV using a secondary electron (SE) detector. The investigations were conducted on fracture surfaces of the specimens after compressive strength testing. Samples were sputtered with gold before the SEM measurements.

The compressive strength tests were performed on a ToniPRAX device at a loading rate of 240 N/s, which is equivalent to 0.6 MPa/s for the investigated specimens (cubes, 20 mm × 20 mm × 20 mm). Testing was always conducted within the first 30 min after removing the samples from the curing regime. Compressive strength was tested after 1 d, 3 d and 7 d of curing.

3. Results and discussion

3.1. Structural investigations

The XRD results for the untreated RHA as well as for the cured geopolymers are shown in Fig. 3. The hump from the RHA, maximum located at 21.82° 2θ, disappeared after curing and a new hump with its maximum at 27.68° 2θ, representing the geopolymeric gel [34], occurred after curing. The disappearance of the hump from the RHA indicates its virtually complete reaction, i.e. a degree of reaction of the RHA close to 100%. This contrasts previously investigated one-part geopolymer systems, in which the silica feedstocks reacted only partly, depending on the initial SiO_2/Al_2O_3 ratio [16,18]. In particular, at a starting SiO_2/Al_2O_3 (i.e. total SiO_2/Al_2O_3 ratio of the mix including silica and sodium aluminate) of ~3.5 mol/mol the degree of reaction of the silica feedstocks (microsilica or silica-rich residue from chlorosilane production) in these previous investigations was only ~55%, while the degree of reaction of the RHA at the same starting SiO_2/Al_2O_3 (Table 2) is near 100%.

The diffractograms of the 1 d, 3 d and 7 d cured specimens indicated almost completely amorphous reaction products. No crystalline aluminosilicates, such as zeolites, were observed; thus the cured mixes can be considered to be pure geopolymers, different to the composite-like character of zeolite-containing one-part systems mentioned above [16,18,19].

Minor amounts of thermonatrite ($Na_2CO_3 \cdot H_2O$; PDF # 00-008-0448) could be identified in the geopolymers, due to minor carbonation of the highly alkaline reaction system. The phosphate and the calcite, present in the starting RHA, disappeared after curing, indicating their dissolution during curing; cristobalite and quartz remained in the system after curing (Fig. 3).

Curing for longer periods than 1 d did not lead to significant changes in the phase content, as observed by XRD. This leads to the conclusion that after one day of curing the geopolymerization reactions were almost complete. This behavior has also been observed with one-part geopolymers based on other silica feedstocks cured at 80 °C [16,18].

The infrared (ATR FT-IR) spectra of the unreacted RHA and the cured geopolymers are shown in Fig. 4. All spectra, particularly the spectra of the cured geopolymers, exhibited broad and overlapping absorption bands, which demonstrates the amorphous character of the compounds.

Bands around 3350 cm^{-1} (vibration 1; numbers refer to designations in Fig. 4) correspond to overlapping asymmetric and symmetric stretching vibrations of the incorporated water and are only present in the geopolymer samples. Their intensity decreased with increasing curing time, indicating a slight water loss during curing, despite the fact that relative humidity was 80%. The same behavior – a decrease in intensity with increasing curing time – was observed for the bending vibration of water (vibration 2). No water bands were observed in the RHA spectrum, consistent with the fact that the material was produced by calcination at 650 °C.

Bands around 1440–1400 cm^{-1} (vibration 3) in the geopolymers are attributed to carbonate [35], i.e. the signals are caused by the incorporated thermonatrite, which has been observed by XRD (Fig. 3). These carbonate absorptions bands were only found in the geopolymer samples, i.e. the marginal amount of calcite in the anhydrous RHA was not observed in its infrared spectrum.

Peaks at 1059 cm^{-1} (vibration 4) and between 985 and 975 cm^{-1} (vibration 5) correspond to asymmetric stretching vibrations of Si-O-Si in the RHA and Si-O-T (T = Si or Al) in the geopolymers, respectively. The absorption bands of asymmetric Si-O-T

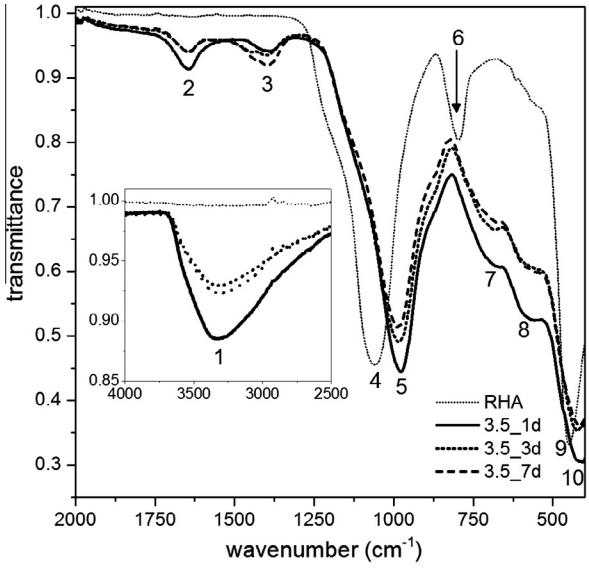

Fig. 4. ATR FT-IR spectra of the RHA feedstock and the one-part geopolymers after 1 d, 3 d and 7 d of curing. (1 = $\nu_{as,s}$ H_2O; 2 = δ H_2O; 3 = carbonate; 4 = ν_{as} Si-O-Si; 5 = ν_{as} Si-O-T (T = Si or Al); 6 = ν_s Si-O-Si; 7 = ν_s Si-O-T (T = Si or Al); 8 = CB (complex band); 9 = δ O-Si-O in RHA; 10 = δ O-Si-O in geopolymers.)

stretching vibrations in tectosilicates shift to lower wavenumbers with increasing aluminum content [36–38]. Therefore, this shift proves the incorporation of aluminum in the geopolymer network.

The Si-O-Si symmetric stretching vibration of the RHA at 797 cm^{-1} (vibration 6) did not remain in the geopolymer samples. Instead, Si-O-T (T = Si or Al) absorptions were observed at 684–680 cm^{-1} (vibration 7). Again, there was a shift to lower wavenumbers and the disappearance of the characteristic vibration 6 (ν_s Si-O-Si) was a further indication of a high degree of reaction of the silica feedstock.

Absorption bands in the range 575–573 cm^{-1} (vibration 8) in the geopolymers are attributed to complex vibrations (CB = complex band) of stretching and bending vibrations (ν_s Si-O-Si; δ O-Si-O) [39]. Bands at 451 cm^{-1} (vibration 9) and at 421–419 cm^{-1} (vibration 10) represent O-Si-O bending vibrations in the RHA feedstock and the geopolymers, respectively.

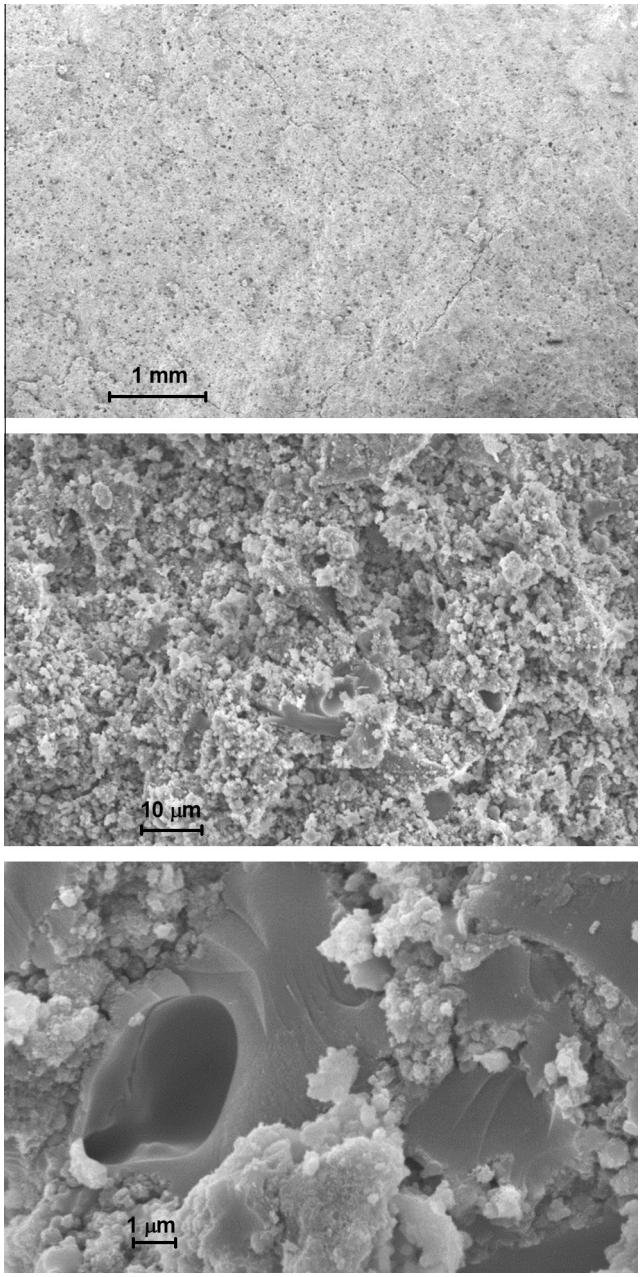

Fig. 5. SEM micrographs of the one-part geopolymers after 3 d of curing.

SEM micrographs of the 3 d cured one-part geopolymer are shown in Fig. 5. At lower magnification (Fig. 5, top), a microstructure comprising homogeneously distributed, small pores, was observed. At higher magnification (Fig. 5, bottom), the geopolymer exhibits mainly the dense and homogeneous microstructure that is observed for well-cured conventional geopolymers (e.g., based on fly ash [40]) too. Besides, the micrograph also shows regions of particulate structure (e.g., bottom middle); these particles are however not remnants of the RHA, as the latter has reacted almost completely.

3.2. Compressive strength

Fig. 6 shows the compressive strengths of the one-part geopolymer after 1, 3 and 7 days of curing. After 1 d the specimens reached compressive strengths of 29.8 MPa on average. After 3 d of curing the average compressive strength reached the maximum value of 32.7 MPa. Curing for 7 d resulted in a slight strength decrease (30.1 MPa). Since the compressive strengths at all investigated curing times were similar, it is concluded that curing times longer than 24 h are of no use for the investigated material at the employed curing conditions.

The obtained strengths are significantly higher than the strengths of one-part geopolymers with similar compositions, but different silica starting materials [16,18,19]. The principal reason for the higher strength of the one-part geopolymers produced from RHA is assumed to be the higher degree of reaction of the silica and the absence of zeolites, as is discussed in more detail in Section 3.3.

3.3. General discussion

Generally, one-part geopolymer mixes tend to form significant amounts of crystalline zeolites as reaction products [11,12,14–19]. In addition, it appears that these mixes often yield products of comparatively low compressive strengths; in the published literature strengths are significantly below 30 MPa or strength data is not reported [11,12,14,16–19]. However, Feng et al. [15] were able to produce one-part geopolymers with a comparatively low amount of incorporated crystallites, which reached compressive strengths of >30 MPa after 7 days of curing at 25 °C. This suggests that avoiding the formation of crystalline byproducts during geopolymerization enhances the strengths of one-part geopolymers.

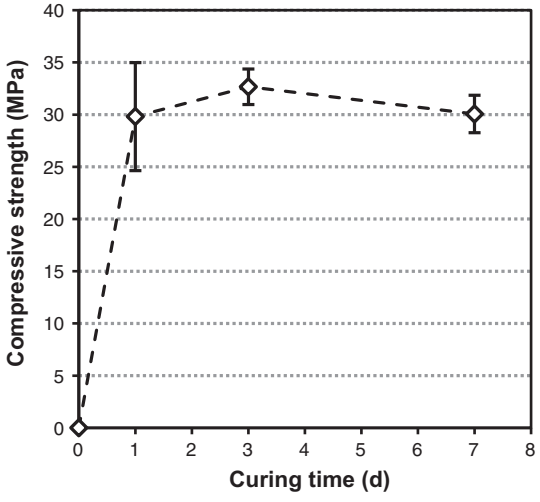

Fig. 6. Compressive strength of the one-part geopolymers after 1 d, 3 d and 7 d of curing. (Error bars represent one standard deviation in each direction.).

It is thus interpreted that the absence of crystalline side-products (zeolites) in the RHA-based geopolymers (Fig. 3) contributed to their higher strength when compared to one-part geopolymers produced from most other feedstocks.

The one-part mixes investigated in Refs. [16,18,19], synthesized in the same way as the formulations investigated in the present contribution, but using microsilica and a residue from chlorosilane production as silica feedstocks, were found to have an silica/alumina-ratio of the reactions products of $SiO_2/Al_2O_3 \approx 2$ mol/mol, independent of the starting mix-design of the pastes [16,18]. In all cases, dissolution of the silica and formation of reaction products ceased when this SiO_2/Al_2O_3 ratio was reached. The silica not consumed to reach this SiO_2/Al_2O_3 ratio remained undissolved in the hardened pastes. In contrast to these previous results, the one-part geopolymers produced from RHA exhibited a virtually complete reaction of the silica feedstock (RHA), as indicated by XRD and ATR FT-IR spectroscopy, and the pastes transformed into amorphous sodium aluminosilicate (N-A-S(-H)) gel, i.e. no zeolites formed. It is known that it is this N-A-S(-H) gel that is mainly responsible for the strength development of low-calcium alkali-activated materials [2,34]. The strength of geopolymers is thus dependent on the amount of N-A-S(-H) gel formed, its composition and its microstructure. As shown in Fig. 5 (bottom) the RHA-based one-part geopolymers exhibited a rather dense and homogeneous microstructure. In contrast, the microstructure of the one-part geopolymers based on the other silica materials (i.e. microsilica or silica residue from chlorosilane production) consists of ca. 100 nm-sized particles, possessing a large amount of interparticle pore space [16,19]. This difference can be attributed to the SiO_2/Al_2O_3 ratio of the geopolymeric gel: In their SEM study on metakaolin- and fly ash-based geopolymers, Steveson and Sagoe-Crentsil [41,42] found that there is a transition from a particulate and porous microstructure at low SiO_2/Al_2O_3 ratios (2.5–3 mol/mol) to a dense and homogeneous microstructure at higher SiO_2/Al_2O_3 ratios (3.5–3.9 mol/mol). Similar observations have been made by Duxson et al. [43]. It can thus be concluded that the high degree of reaction of the RHA led to a comparatively high SiO_2/Al_2O_3 ratio of the reacted geopolymer (presumably in the range of the starting SiO_2/Al_2O_3 of ~3.5 mol/mol; Table 2) and consequently to a denser microstructure than in other one-part geopolymers, which caused a higher compressive strength of the RHA-based material.

Summarizing, we attribute the comparatively high compressive strengths of the RHA-based one-part geopolymers mainly to (1) the absence of significant amounts of crystalline byproducts, and (2) the almost complete reaction of the RHA, which resulted in a higher SiO_2/Al_2O_3 ratio and a denser microstructure of the N-A-S(-H) gel than in one-part geopolymers produced from other silica sources.

Other factors that probably also contributed to the comparatively high compressive strength of the RHA-based one-part geopolymers were: (1) the absence of swelling of the hardening paste, contrary to observations made on some one-part geopolymers based on microsilica or other silica-rich by-products [19], and (2) a better workability of the RHA-based pastes as compared to pastes based on the other aforementioned silica feedstocks, which can lead to less inhomogeneities in the paste and thus in the hardened geopolymer. The latter observation is attributed to different particle characteristics of the RHA: The particle size distribution as measured by laser granulometry (d_{50} = 11.1 μm; d_{90} = 39.8 μm; Fig. 1) of the RHA was significantly coarser than the particle size distributions of previously investigated silica feedstocks – microsilica and a residue from chlorosilane production, which had $d_{50} \approx 0.2$–1.0 μm and 6.8 μm, respectively [16,18]. In addition, these other silica feedstocks consisted of particles composed of small ($d \approx 100$–200 nm) primary particles, causing a high intraparticle porosity, which increases the water demand of the pastes and leads to a poorer workability.

Despite its coarser PSD, the RHA had a higher specific surface area (49.6 m^2/g) than the microsilica and the residue from chlorosilane production (20.1 m^2/g and 32.3 m^2/g, respectively). This can be explained by the fact that the particles of the RHA had a more angular shape, apparently a rougher surface (cf. Fig. 2) and a significant amount of mesopores (average pore diameter ~12.9 nm; see Section 2.1) when compared to the particles of microsilica and similar materials. This higher specific surface area of the RHA is assumed to be a major reason for the higher degree of reaction of the RHA when compared to the other silica feedstocks.

4. Conclusions

One-part geopolymers were produced from rice husk ash (RHA) by mixing the RHA with solid sodium aluminate at a ratio to yield SiO_2/Al_2O_3 = 3.5 and subsequently mixing the solid blend with water and curing at 80 °C and 80% r.H. The compressive strength of the geopolymer was ~30 MPa after one day of curing. As shown by XRD, the feedstocks almost completely reacted and transformed into amorphous geopolymer (N-A-S(-H) gel). Comparison of the infrared spectra of the RHA and the reaction products indicated a high degree of reaction of the RHA too. No crystalline reaction products were observed, except for minor amounts of hydrated sodium carbonate due to carbonation. Curing for longer times than one day caused a slight decrease of the water content of the geopolymer, but no other significant changes were observed in the XRD patterns and the infrared spectra.

The results of this study thus show that RHA can be applied successfully for the synthesis of one-part geopolymers. The RHA-based geopolymers provide some improved properties when compared to one-part geopolymers based on other silica materials, in particular an almost complete reaction of the silica feedstock and a comparatively high compressive strength. Optimization of the RHA-based one-part geopolymers regarding chemical composition and water/binder ratio, as well as curing conditions and curing times will be subject of future studies.

Acknowledgements

The authors thank Christiane Weimann and Carsten Prinz for help with the SEM investigations and the determination of specific surface area and porosity of the RHA, respectively. The authors are also very grateful to Nsesheye Msinjili for providing the rice husk ash sample. P.S. acknowledges financial support from BAM within the MIS program (proposal Ideen_2012_36).

References

[1] P. Duxson, A. Fernández-Jiménez, J.L. Provis, G.C. Lukey, A. Palomo, J.S.J. van Deventer, Geopolymer technology: the current state of the art, J. Mater. Sci. 42 (2007) 2917–2933.
[2] J.L. Provis, S.A. Bernal, Geopolymers and related alkali-activated materials, Annu. Rev. Mater. Res. 44 (2014) 299–327.
[3] S.A. Bernal, E.D. Rodríguez, A.P. Kirchheim, J.L. Provis, Management and valorisation of wastes through use in producing alkali-activated cement materials, J. Chem. Technol. Biotechnol. 91 (2016) 2365–2388.
[4] C. Gunasekara, D.W. Law, S. Setunge, Long term permeation properties of different fly ash geopolymer concretes, Constr. Build. Mater. 124 (2016) 352–362.
[5] M. Babaee, A. Castel, Chloride-induced corrosion of reinforcement in low-calcium fly ash-based geopolymer concrete, Cem. Concr. Res. 88 (2016) 96–107.
[6] X. Gao, Q.L. Yu, H.J.H. Brouwers, Reaction kinetics, gel character and strength of ambient temperature cured alkali activated slag-fly ash blends, Constr. Build. Mater. 80 (2015) 105–115.
[7] K. Dombrowski, M. Weil, A. Buchwald (Geopolymere Bindemittel. Teil 2: Entwicklung und Optimierung von Geopolymerbetonmischungen für feste und dauerhafte Außenwandbauteile), ZKG Int. 61 (3) (2008) 70–80.

[8] R. Pouhet, M. Cyr, Alkali-silica reaction in metakaolin-based geopolymer mortar, Mater. Struct. 48 (2015) 571–583.
[9] M.C. Bignozzi, S. Manzi, M.E. Natali, W.D.A. Rickard, A. van Riessen, Room temperature alkali activation of fly ash: effect of Na_2O/SiO_2 ratio, Constr. Build. Mater. 69 (2014) 262–270.
[10] W.D.A. Rickard, G.J.G. Gluth, K. Pistol, In-situ thermo-mechanical testing of fly ash geopolymer concretes made with quartz and expanded clay aggregates, Cem. Concr. Res. 80 (2016) 33–43.
[11] D. Koloušek, J. Brus, M. Urbanova, J. Andertova, V. Hulinsky, J. Vorel, Preparation, structure and hydrothermal stability of alternative (sodium silicate-free) geopolymers, J. Mater. Sci. 42 (2007) 9267–9275.
[12] A. Hajimohammadi, J.L. Provis, J.S.J. van Deventer, One-part geopolymer mixes from geothermal silica and sodium aluminate, Ind. Eng. Chem. Res. 47 (2008) 9396–9405.
[13] P. Duxson, J.L. Provis, Designing precursors for geopolymer cements, J. Am. Ceram. Soc. 91 (2008) 3864–3869.
[14] S.J. O'Connor, K.J.D. MacKenzie, Synthesis, characterisation and thermal behaviour of lithium aluminosilicate inorganic polymers, J. Mater. Sci. 45 (2010) 3707–3713.
[15] D. Feng, J.L. Provis, J.S.J. van Deventer, Thermal activation of albite for the synthesis of one-part mix geopolymers, J. Am. Ceram. Soc. 95 (2012) 565–572.
[16] G.J.G. Gluth, C. Lehmann, K. Rübner, H.-C. Kühne, Geopolymerization of a silica residue from waste treatment of chlorosilane production, Mater. Struct. 46 (2013) 1291–1298.
[17] X. Ke, S.A. Bernal, N. Ye, J.L. Provis, J. Yang, One-part geopolymers based on thermally treated red mud/NaOH blends, J. Am. Ceram. Soc. 98 (2015) 5–11.
[18] P. Sturm, S. Greiser, G.J.G. Gluth, C. Jäger, H.J.H. Brouwers, Degree of reaction and phase content of silica-based one-part geopolymers investigated using chemical and NMR spectroscopic methods, J. Mater. Sci. 50 (2015) 6768–6778.
[19] P. Sturm, G.J.G. Gluth, S. Simon, H.J.H. Brouwers, H.-C. Kühne, The effect of heat treatment on the mechanical and structural properties of one-part geopolymer-zeolite composites, Thermochim. Acta 635 (2016) 41–58.
[20] J. He, Synthesis and characterization of geopolymers for infrastructural applications (Ph.D. thesis), Louisiana State University, Baton Rouge, 2012.
[21] FAO Statistical Yearbook – World Food and Agriculture, Food and Agriculture Organization of the United Nations, Rome, 2013, p. 2013.
[22] D. Koteswara Rao, P.R.T. Pranav, M. Anusha, Stabilization of expansive soil with rice husk ash, lime and gypsum – an experimental study, Int. J. Eng. Sci. Technol. 3 (2011) 8076–8085.
[23] S. Chanddrasekhar, K.G. Satyanarayana, P.N. Pramada, Processing, properties and applications of reactive silica from rice husk—an overview, J. Mater. Sci. 38 (2003) 3159–3168.
[24] Y. Shinohara, N. Kohyama, Quantitative analysis of tridymite and cristobalite crystallized in rice husk ash by heating, Ind. Health 42 (2004) 277–285.
[25] D.V. Reddy, M. Alvarez, Marine durability characteristics of rice husk ash-modified reinforced concrete, in: International Latin American and Caribbean Conference for Engineering and Technology, Mayagüez, Puerto Rico, 2006.
[26] G. Abood Habeeb, H. Bin Mahmud, Study on properties of rice husk ash and its use as cement replacement material, Mater. Res. 13 (2010) 185–190.
[27] G. Rodríguez de Sensale, Effect of rice-husk ash on durability of cementitious materials, Cem. Concr. Compos. 32 (2010) 718–725.
[28] G. Chagas Cordeiro, R. Dias Toledo Filho, L.M. Tavares, E. de Moraes Rego Fairbairn, S. Hempel, Influence of particle size and specific surface area on the pozzolanic activity of residual rice husk ash, Cem. Concr. Compos. 33 (2011) 529–534.
[29] V.-T.-A. Van, C. Rößler, D.-D. Bui, H.-M. Ludwig, Rice husk ash as both pozzolanic admixture and internal curing agent in ultra-high performance concrete, Cem. Concr. Compos. 53 (2014) 270–278.
[30] S.A. Bernal, E.D. Rodríguez, R. Mejia de Gutiérrez, J.L. Provis, S. Delvasto, Activation of metakaolin/slag blends using alkaline solutions based on chemically modified silica fume and rice husk ash, Waste Biomass Valoriz. 3 (2012) 99–108.
[31] J. He, Y. Jie, J. Zhang, Y. Yu, G. Zhang, Synthesis and characterization of red mud and rice husk ash-based geopolymer composites, Cem. Concr. Compos. 37 (2013) 108–118.
[32] J.M. Meija, R. Mejia de Gutierrez, F. Puertas, Rice husk ash as a source of silica in alkali-activated fly ash and granulated blast furnace slag systems, Mater. Constr. 63 (2013) 361–375.
[33] U.H. Heo, K. Sankar, W.M. Kriven, S.S. Musil, Rice husk ash as a silica source in a geopolymer formulation, Ceram. Eng. Sci. Proc. 35 (8) (2015) 87–101.
[34] J.L. Provis, G.C. Lukey, J.S.J. van Deventer, Do geopolymers actually contain nanocrystalline zeolites? A reexamination of existing results, Chem. Mater. 17 (2005) 3075–3085.
[35] W.B. White, The carbonate minerals, in: V.C. Farmer (Ed.), The Infrared Spectra of Minerals, Mineralogical Society, London, 1974, pp. 227–284.
[36] H.H.W. Moenke, Silica, the three-dimensional silicates, borosilicates and beryllium silicates, in: V.C. Farmer (Ed.), The Infrared Spectra of Minerals, Mineralogical Society, London, 1974, pp. 365–382.
[37] S. Jakobbson, Determination of Si/Al ratios in semicrystalline aluminosilicates by FT-IR spectroscopy, Appl. Spectrosc. 56 (2002) 797–799.
[38] W. Mozgawa, W. Jastrębski, M. Handke, Vibrational spectra of D4R and D6R structural units, J. Mol. Struct. 744–747 (2005) 663–670.
[39] W. Mozgawa, M. Król, K. Barczyk, FT-IR studies of zeolites from different structural groups, Chemik (2011) 671–674.
[40] W.D.A. Rickard, J. Temuujin, A. van Riessen, Thermal analysis of geopolymer pastes synthesised from five fly ashes of variable composition, J. Non-Cryst. Solids 358 (2012) 1830–1839.
[41] M. Steveson, K. Sagoe-Crentsil, Relationships between composition, structure and strength of inorganic polymers. Part I—Metakaolin-derived inorganic polymers, J. Mater. Sci. 40 (2005) 2023–2036.
[42] M. Steveson, K. Sagoe-Crentsil, Relationships between composition, structure and strength of inorganic polymers. Part 2—fly ash-derived inorganic polymers, J. Mater. Sci. 40 (2005) 4247–4259.
[43] P. Duxson, J.L. Provis, G.C. Lukey, S.W. Mallicoat, W.M. Kriven, J.S.J. van Deventer, Understanding the relationship between geopolymer composition, microstructure and mechanical properties, Colloids Surf. A 269 (2005) 47–58.